

A Twistor Approach to One-Loop Amplitudes in $\mathcal{N}=1$ Supersymmetric Yang-Mills Theory

James Bedford, Andreas Brandhuber, Bill Spence and Gabriele Travaglini ¹

*Department of Physics
Queen Mary, University of London
Mile End Road, London, E1 4NS
United Kingdom*

Abstract

We extend the twistor string theory inspired formalism introduced in hep-th/0407214 for calculating loop amplitudes in $\mathcal{N}=4$ super Yang-Mills theory to the case of $\mathcal{N}=1$ (and $\mathcal{N}=2$) super Yang-Mills. Our approach yields a novel representation of the gauge theory amplitudes as dispersion integrals, which are surprisingly simple to evaluate. As an application we calculate one-loop maximally helicity violating (MHV) scattering amplitudes with an arbitrary number of external legs. The result we obtain agrees precisely with the expressions for the $\mathcal{N}=1$ MHV amplitudes derived previously by Bern, Dixon, Dunbar and Kosower using the cut-constructibility approach.

¹{j.a.p.bedford, a.brandhuber, w.j.spence, g.travaglini}@qmul.ac.uk

1 Introduction

In a remarkable paper [1] it was proposed that perturbative $\mathcal{N} = 4$ super Yang-Mills (SYM) is dual to the topological B model on super twistor space $\mathbb{CP}^{3|4}$. Interestingly, this duality relates the perturbative expansion of gauge theory amplitudes to a D1-brane instanton expansion on the string theory side. The relevant instantons correspond to algebraic curves embedded holomorphically in super twistor space. Their degree d and genus g are related to the number of negative helicity gluons q and number of loops l of the amplitude as $d = q - 1 + l$ and $g \leq l$.

In [1] the maximally helicity violating (MHV) tree amplitudes [2, 3] were reproduced directly from a computation in the B model with $d = 1$, $g = 0$ curves. For more general amplitudes the story becomes more involved, since in [1] it was already pointed out that in principle both connected and disconnected instantons can contribute to a given amplitude. The approach using connected instantons was pursued further in [4–6], and agreement with existing results was found. On the other hand, [7] introduced a new diagrammatic method to calculate tree-level amplitudes using MHV amplitudes as effective vertices after a suitable off-shell continuation. This method is related to the string theory approach using contributions from completely disconnected instantons only, and is extremely efficient for calculating tree amplitudes. The authors of [8] argued that both computations are equivalent, and that the instanton contributions localize on singular curves corresponding to intersecting “lines”, i.e. degree one curves in twistor space.

The method of [7] led to a rederivation of previously known results in a much faster way, and also allowed the calculation of new scattering amplitudes with increasing helicity violation as well as with fermionic and scalar external particles [9]–[16]. The next logical question to ask was clearly whether this procedure could be extended to the calculation of amplitudes at loop level. This question was positively answered by three of the present authors in [17], where it was shown how to combine MHV vertices into loop diagrams in $\mathcal{N} = 4$ SYM theory. The result was a new representation of the scattering amplitudes in terms of dispersive integrals which, rather surprisingly, proved to be tractable, and led to perfect agreement with the expressions for the one-loop MHV scattering amplitudes in $\mathcal{N} = 4$ SYM previously obtained by Bern, Dixon, Dunbar and Kosower (BDDK) in [18] using the cut-constructibility approach. As a bonus, the analysis of [17] gave a novel representation of the “easy two-mass” (2me) scalar box function, containing one less dilogarithm and one less logarithm than the traditional one of BDDK.

The twistor string theory originally proposed in [1] and other versions proposed in [19, 20] cannot reproduce gauge theory amplitudes at loop level [21], due to the fact that conformal supergravity fields propagate in the loops. Nevertheless, one can study known loop amplitudes to extract information about their localisation properties in twistor space. This was done in [22] for supersymmetric MHV one-loop amplitudes (and some non-supersymmetric amplitudes), and localisation was indeed found onto three types of

diagrams. The twistor space picture suggested by the result of [17] differed from that of [22], in that one of the class of diagrams proposed in the analysis of [22] is absent. The resolution of this discrepancy was recently [23] linked to a subtlety in the use of the differential operators employed to establish localisation, and led to the appearance of a “holomorphic anomaly”. With this taken into account, it was shown in [23] that, as far as the one-loop $\mathcal{N} = 4$ SYM amplitudes are concerned, the expectations from [17] are confirmed and the one-loop MHV amplitudes in $\mathcal{N} = 4$ localise on pairs of lines in twistor space which are joined by two twistor space propagators. The holomorphic anomaly was evaluated explicitly in [24,25], and twistor space localisation was further elucidated in [24] by transforming the results of [7] and [17] directly to twistor space. Furthermore, the holomorphic anomaly was recently exploited as a new tool for deriving one-loop next-to-MHV amplitudes in $\mathcal{N} = 4$ SYM [25,26] in combination with the powerful cut-constructibility approach. These and other new one-loop amplitudes in $\mathcal{N} = 4$ SYM were recently derived in [27] using cut-constructibility.

It now appears plausible that the entire quantum theory of $\mathcal{N} = 4$ SYM will have a description based upon the MHV diagram approach, which in turn reflects the properties of localisation in twistor space. Moreover, we now have direct methods to test this, using MHV vertices assembled into MHV diagrams according to well-defined rules. We expect further evidence to emerge with the continuing study of non-MHV tree and one-loop amplitudes, as well as higher-loop amplitudes. It should be fairly straightforward to check that the few remaining existing results that have so far not been obtained by these new methods are reproduced.

We find it intriguing that, although the twistor string/gauge theory correspondence is spoiled at loop level, one can still use MHV vertices and combine them to obtain the correct $\mathcal{N} = 4$ SYM loop amplitudes [17]. Perhaps even more surprisingly, we will show in this paper that the applicability of the method of [17] actually holds for theories with less supersymmetry as well, which are interesting not least for potential applications to phenomenology. Specifically, in this paper we will obtain one-loop MHV amplitudes in $\mathcal{N} = 1$ SYM by combining MHV vertices into one-loop diagrams following the procedure proposed in [17]. The result we find agrees perfectly with the BDDK computation of [28].²

The rest of this paper is organised as follows. In Section 2 we begin by reviewing the expression for the one-loop MHV scattering amplitudes in $\mathcal{N} = 1$ SYM derived by BDDK in [28]. There, we also present a slightly simplified version of the BDDK result which will be useful in making the comparison with the results derived from MHV vertices. Section 3 reviews relevant aspects of the work of [17], thereby establishing the set-up for the calculation of loop amplitudes with MHV vertices. In Section 4 we turn to the formulation and explicit calculation of the one-loop MHV amplitudes in $\mathcal{N} = 1$ SYM. Finally, in three Appendices we summarise some technical results which are required in the course of the calculations presented in Section 4.

²The arguments presented here also apply directly to $\mathcal{N} = 2$ SYM.

2 The $\mathcal{N} = 1$ MHV amplitudes at one loop

The expression for the MHV amplitudes at one loop in $\mathcal{N} = 1$ SYM was obtained for the first time by BDDK in [28], using the cut-constructibility method. We will shortly give their explicit result, and then simplify it by introducing appropriate functions. This turns out to be useful when we compare the BDDK result to that which we will derive by using MHV diagrams.

In order to obtain the one-loop MHV amplitudes in $\mathcal{N} = 1$ and $\mathcal{N} = 2$ SYM it is sufficient to compute the contribution $\mathcal{A}_n^{\mathcal{N}=1, \text{chiral}}$ to the one-loop MHV amplitudes coming from a single $\mathcal{N} = 1$ chiral multiplet. This was calculated in [28], and the result turns out to be proportional to the Parke-Taylor MHV tree amplitude [2]

$$\mathcal{A}_n^{\text{tree}} := \frac{\langle ij \rangle^4}{\prod_{k=1}^n \langle k k+1 \rangle}, \quad (2.1)$$

as is also the case with the one-loop MHV amplitudes in $\mathcal{N} = 4$ SYM. However, in contradistinction with that case, the remaining part of the $\mathcal{N} = 1$ amplitudes depends non-trivially on the position of the negative helicity gluons i and j . The result obtained in [28] is:

$$\begin{aligned} \mathcal{A}_n^{\mathcal{N}=1, \text{chiral}} &= \mathcal{A}_n^{\text{tree}} \cdot \left\{ \sum_{m=i+1}^{j-1} \sum_{s=j+1}^{i-1} b_{m,s}^{i,j} B(t_{m+1}^{[s-m]}, t_m^{[s-m]}, t_{m+1}^{[s-m-1]}, t_{s+1}^{[m-s-1]}) \right. \\ &+ \sum_{m=i+1}^{j-1} \sum_{a \in \mathcal{D}_m} c_{m,a}^{i,j} \frac{\log(t_{m+1}^{[a-m]}/t_m^{[a-m+1]})}{t_{m+1}^{[a-m]} - t_m^{[a-m+1]}} + \sum_{m=j+1}^{i-1} \sum_{a \in \mathcal{C}_m} c_{m,a}^{i,j} \frac{\log(t_{a+1}^{[m-a]}/t_{a+1}^{[m-a-1]})}{t_{a+1}^{[m-a]} - t_{a+1}^{[m-a-1]}} \\ &\left. + \frac{c_{i+1,i-1}^{i,j}}{t_i^{[2]}} K_0(t_i^{[2]}) + \frac{c_{i-1,i}^{i,j}}{t_{i-1}^{[2]}} K_0(t_{i-1}^{[2]}) + \frac{c_{j+1,j-1}^{i,j}}{t_j^{[2]}} K_0(t_j^{[2]}) + \frac{c_{j-1,j}^{i,j}}{t_{j-1}^{[2]}} K_0(t_{j-1}^{[2]}) \right\}, \end{aligned} \quad (2.2)$$

where $t_i^{[k]} := (p_i + p_{i+1} + \dots + p_{i+k-1})^2$ for $k \geq 0$, and $t_i^{[k]} = t_i^{[n-k]}$ for $k < 0$. The sums in the second line of (2.2) cover the ranges \mathcal{C}_m and \mathcal{D}_m defined by

$$\mathcal{C}_m = \begin{cases} \{i, i+1, \dots, j-2\}, & m = j+1, \\ \{i, i+1, \dots, j-1\}, & j+2 \leq m \leq i-2, \\ \{i+1, i+2, \dots, j-1\}, & m = i-1, \end{cases} \quad (2.3)$$

and

$$\mathcal{D}_m = \begin{cases} \{j, j+1, \dots, i-2\}, & m = i+1, \\ \{j, j+1, \dots, i-1\}, & i+2 \leq m \leq j-2, \\ \{j+1, j+2, \dots, i-1\}, & m = j-1. \end{cases} \quad (2.4)$$

The coefficients $b_{m,s}^{i,j}$ and $c_{m,a}^{i,j}$ are

$$b_{m,s}^{i,j} := -2 \frac{\text{tr}_+(k_i k_j k_m k_s) \text{tr}_+(k_i k_j k_s k_m)}{[(k_i + k_j)^2]^2 [(k_m + k_s)^2]^2}, \quad (2.5)$$

$$c_{m,a}^{i,j} := \left[\frac{\text{tr}_+(k_m k_{a+1} k_j k_i)}{(k_{a+1} + k_m)^2} - \frac{\text{tr}_+(k_m k_a k_j k_i)}{(k_a + k_m)^2} \right] \frac{\text{tr}_+(k_i k_j k_m q_{m,a}) - \text{tr}_+(k_i k_j q_{m,a} k_m)}{[(k_i + k_j)^2]^2}, \quad (2.6)$$

where $q_{r,s} := \sum_{l=r}^s k_l$. Notice that both coefficients $b_{m,s}^{i,j}$ and $c_{m,a}^{i,j}$ are symmetric under the exchange of i and j . In the case of b this is evident; for c , this is also manifest as it is expressed as the product of two antisymmetric quantities. The function B in the first line

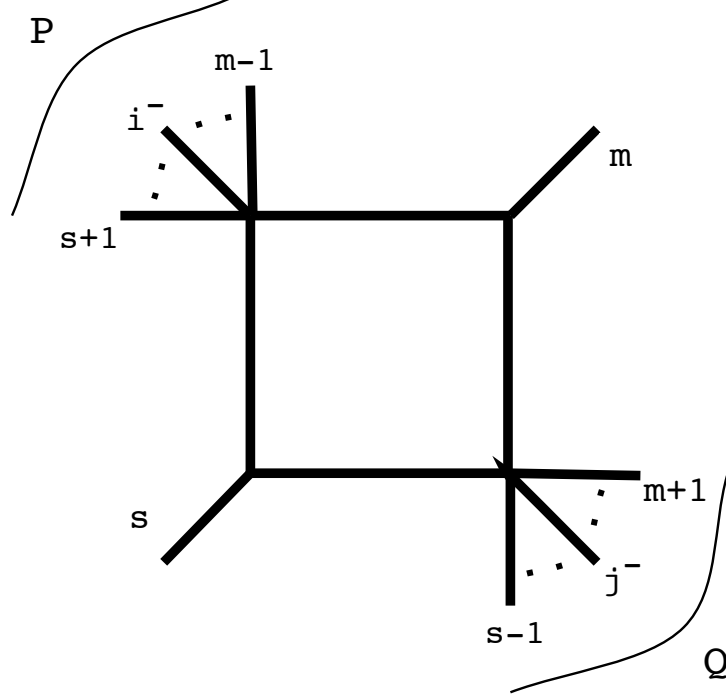


Figure 1: The box function F of (2.7), whose finite part B , Eq. (2.9), appears in the $\mathcal{N} = 1$ amplitude (2.2). The two external gluons with negative helicity are labelled by i and j . The legs labelled by s and m correspond to the null momenta p and q respectively in the notation of (2.9). Moreover, the quantities $t_{m+1}^{[s-m]}$, $t_m^{[s-m]}$, $t_{m+1}^{[s-m-1]}$, $t_{s+1}^{[m-s-1]}$ appearing in the box function B in (2.19) correspond to the kinematical invariants $t := (Q + p)^2$, $s := (P + p)^2$, Q^2 , P^2 in the notation of (2.9), with $p + q + P + Q = 0$.

of (2.2) is the “finite” part of the easy two-mass (2me) scalar box function $F(s, t, P^2, Q^2)$, with

$$F(s, t, P^2, Q^2) := -\frac{1}{\epsilon^2} \left[(-s)^{-\epsilon} + (-t)^{-\epsilon} - (-P^2)^{-\epsilon} - (-Q^2)^{-\epsilon} \right] + B(s, t, P^2, Q^2). \quad (2.7)$$

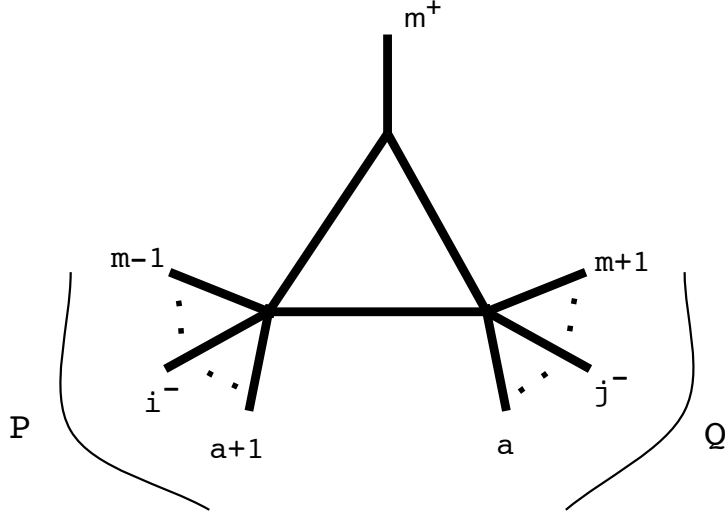


Figure 2: A triangle function, corresponding to the first term $T_\epsilon(p_m, q_{a+1, m-1}, q_{m+1, a})$ in the second line of (2.19). p , Q and P correspond to p_m , $q_{m+1, a}$ and $q_{a+1, m-1}$ in the notation of Eq. (2.19), where $j \in Q$, $i \in P$. In particular, $Q^2 \rightarrow t_{m+1}^{[a-m]}$ and $P^2 \rightarrow t_m^{[a-m+1]}$.

As in [17], we have introduced the following convenient kinematical invariants:

$$s := (P + p)^2, \quad t := (P + q)^2, \quad (2.8)$$

where p and q are null momenta, and P and Q are in general massive, with $p + q + P + Q = 0$.³ In [17] the following new expression for B was found:

$$B(s, t, P^2, Q^2) = \text{Li}_2(1 - aP^2) + \text{Li}_2(1 - aQ^2) - \text{Li}_2(1 - as) - \text{Li}_2(1 - at), \quad (2.9)$$

where

$$a = \frac{P^2 + Q^2 - s - t}{P^2 Q^2 - st}. \quad (2.10)$$

The expression (2.9) contains one less dilogarithm and one less logarithm than the traditional form used by BDDK,

$$\begin{aligned} B(s, t, P^2, Q^2) &= \text{Li}_2\left(1 - \frac{P^2}{s}\right) + \text{Li}_2\left(1 - \frac{P^2}{t}\right) + \text{Li}_2\left(1 - \frac{Q^2}{s}\right) + \text{Li}_2\left(1 - \frac{Q^2}{t}\right) \\ &\quad - \text{Li}_2\left(1 - \frac{P^2 Q^2}{st}\right) + \frac{1}{2} \log^2\left(\frac{s}{t}\right). \end{aligned} \quad (2.11)$$

³The kinematical invariant $s = (P + p)^2$ should not be confused with the label s which is also used to label an external leg (as in Figure 1 for example). The correct meaning will be clear from the context.

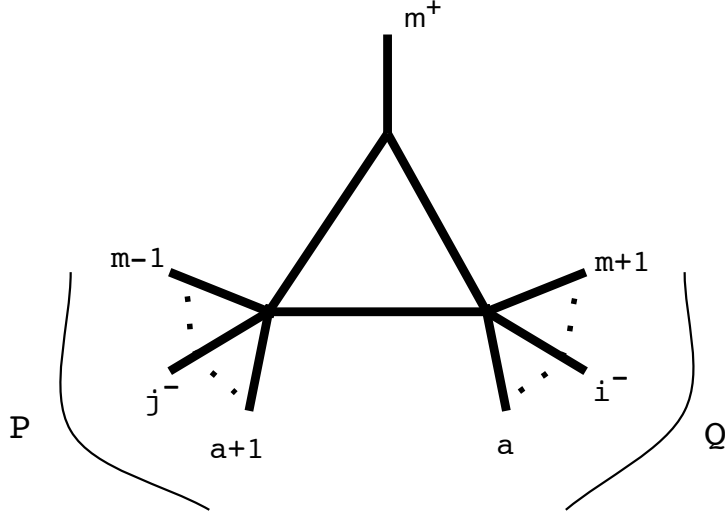


Figure 3: *This triangle function corresponds to the second term in the second line of (2.19) – where i and j are swapped. As in Figure 2, p , Q and P correspond to p_m , $q_{m+1,a}$ and $q_{a+1,m-1}$ in the notation of Eq. (2.19), where now $i \in Q$, $j \in P$. In particular, $Q^2 \rightarrow t_{a+1}^{[m-a]}$ and $P^2 \rightarrow t_{a+1}^{[m-a-1]}$.*

The agreement of (2.9) with (2.11) was discussed and proved in Section 5 of [17].⁴ In Figure 1 we give a pictorial representation of the box function F defined in (2.7) (with the leg labels identified by $s \rightarrow p$, $m \rightarrow q$).

Finally, infrared divergences are contained in the bubble functions $K_0(t)$, defined by

$$K_0(t) := \frac{(-t)^{-\epsilon}}{\epsilon(1-2\epsilon)}. \quad (2.12)$$

We notice that in order to re-express (2.2) in a simpler form, it is useful to introduce the triangle function [22]

$$T(p, P, Q) := \frac{\log(Q^2/P^2)}{Q^2 - P^2}, \quad (2.13)$$

with $p + P + Q = 0$. A diagrammatic representation of this function is given in Figure 2

⁴More precisely, this agreement holds only in certain kinematical regimes e.g. in the Euclidean region where all kinematical invariants are negative. More care is needed when analytically continuing the amplitude to the physical region. The usual prescription of replacing a kinematical invariant s by $s + i\epsilon$ and continuing s from negative to positive values gives the correct result only for our form of the box function (2.9), whereas (2.11) has to be amended by correction terms [29].

(with $m^+ \rightarrow p$). We also find it useful to introduce an ϵ -dependent triangle function,⁵

$$T_\epsilon(p, P, Q) := \frac{1}{\epsilon} \frac{(-P^2)^{-\epsilon} - (-Q^2)^{-\epsilon}}{Q^2 - P^2}. \quad (2.14)$$

As long as P^2 and Q^2 are non-vanishing, one has

$$\lim_{\epsilon \rightarrow 0} T_\epsilon(p, P, Q) = T(p, P, Q), \quad P^2 \neq 0, Q^2 \neq 0. \quad (2.15)$$

If either of the invariants vanishes, one has a different limit. For example, if $Q^2 = 0$, one has

$$T_\epsilon(p, P, Q)|_{Q^2=0} \longrightarrow -\frac{1}{\epsilon} \frac{(-P^2)^{-\epsilon}}{P^2}, \quad \epsilon \rightarrow 0. \quad (2.16)$$

We will call these cases “degenerate triangles”.

The usefulness of the previous remark stems from the fact that precisely the quantity $(1/\epsilon) \cdot [(-P^2)^{-\epsilon}/P^2]$ appears in the last line of (2.2) – the bubble contributions. Therefore, these can be equivalently obtained as degenerate triangles, i.e. triangles where one of the massive legs becomes massless.

Specifically, we notice that the four degenerate triangles (bubbles) in the last line of (2.2) can be precisely obtained by including the “missing” index assignments in \mathcal{D}_m and \mathcal{C}_m :

$$(m = i + 1, a = i - 1), \quad (m = j - 1, a = j) \quad \text{for } \mathcal{D}_m, \quad (2.17)$$

which correspond to two degenerate triangles, and

$$(m = j + 1, a = j - 1), \quad (m = i - 1, a = i) \quad \text{for } \mathcal{C}_m, \quad (2.18)$$

corresponding to two more degenerate triangles.

In conclusion, the previous remarks allow us to rewrite (2.2) in a more compact form as follows:

$$\begin{aligned} \mathcal{A}_n^{\mathcal{N}=1, \text{chiral}} &= \mathcal{A}_n^{\text{tree}} \cdot \left\{ \sum_{m=i+1}^{j-1} \sum_{s=j+1}^{i-1} b_{m,s}^{i,j} B(t_{m+1}^{[s-m]}, t_m^{[s-m]}, t_{m+1}^{[s-m-1]}, t_{s+1}^{[m-s-1]}) \right. \\ &\quad \left. + \frac{1}{1-2\epsilon} \left[\sum_{m=i+1}^{j-1} \sum_{a=j}^{i-1} c_{m,a}^{i,j} T_\epsilon(p_m, q_{a+1, m-1}, q_{m+1, a}) + (i \longleftrightarrow j) \right] \right\}. \end{aligned} \quad (2.19)$$

In the previous expression it is understood that we only keep terms that survive in the limit $\epsilon \rightarrow 0$. This means that the factor $1/(1-2\epsilon)$ can be replaced by 1 whenever the term in the sum is finite, i.e. whenever the triangle is non-degenerate. However, in the case of

⁵The function $T_\epsilon(p, P, Q)$ defined in (2.14) arises naturally in the twistor-inspired approach which will be developed in Sections 3 and 4.

degenerate triangles, which contain infrared divergent terms, we have to expand this factor to linear order in ϵ . In the notation of (2.19), $q_{m+1,a}^2 = t_{m+1}^{[a-m]}$ and $q_{a+1,m-1}^2 = t_m^{[a-m+1]}$; in Figure 2, these invariants correspond to Q^2 and P^2 respectively, where $j \in Q$, $i \in P$. In the sum with $i \leftrightarrow j$, one would have $q_{m+1,a}^2 = t_{a+1}^{[m-a]}$, $q_{a+1,m-1}^2 = t_{a+1}^{[m-a-1]}$, corresponding respectively to Q^2 and P^2 in Figure 3, with $i \in Q$, $j \in P$. It is the expression (2.19) for the $\mathcal{N} = 1$ chiral multiplet amplitude which we will derive using MHV diagrams.

3 A brief review of loop diagrams from MHV vertices

In this Section we briefly review the method proposed in [17] to compute loop amplitudes in supersymmetric gauge theories, referring the reader to Sections 3–5 of that paper for a more detailed discussion of this procedure, as well as for an example of its application to the calculation of one-loop MHV amplitudes in $\mathcal{N} = 4$ SYM.

Before starting, let us first recall that in what follows we will be dealing with the so-called colour-stripped or partial amplitudes. More specifically, for an n -particle scattering amplitude we will compute the term proportional to $\text{Tr}(T^{a_1} \dots T^{a_n})$, where the T^a 's are the generators of the gauge group. The full planar amplitude is then obtained by summing over non-cyclic permutations. It is a remarkable result of BDDK that, at one loop, non-planar amplitudes are simply obtained as a sum over permutations of the planar ones. This is discussed in Section 7 of [18], where it was also noted that this applies to a generic theory with adjoint particles running in the loops, such as $\mathcal{N} = 1, 2, 4$ SYM. At the level of group theory factors, the diagrammatics for building one-loop MHV amplitudes in the BDDK cut-constructibility approach and in the approach discussed in this paper (as well as in [17], for the $\mathcal{N} = 4$ case) are precisely the same. Hence, the agreement at one loop between the two methods at planar level in fact trivially extends to subleading corrections in $1/N$.

We now come back to the description of the approach of [17] to loop amplitudes. The procedure used there was:

1. Lift the MHV tree-level scattering amplitudes to vertices, by continuing the internal lines off shell using a prescription equivalent to that of CSW. Internal lines are then connected by scalar propagators which join particles of the same spin but opposite helicity.
2. Build MHV diagrams with the required external particles at loop level using the MHV tree-level vertices, and sum over all independent diagrams obtained in this fashion for a fixed ordering of external helicity states.
3. Re-express the loop integration measure in terms of the off-shell parametrisation employed for the loop momenta.

4. Analytically continue to $4-2\epsilon$ dimensions in order to deal with infrared divergences, and perform all loop integrations.

Using this method, we will show in Section 4 that combining MHV vertices into one-loop diagrams precisely yields the results for the contribution of the chiral multiplet to MHV amplitudes, as obtained by BDDK using the cut-constructibility approach.

We start off by discussing the off-shell continuation which was used in [17], and found to be very useful for calculating loop diagrams. Consider a generic off-shell momentum vector, L . On general grounds, it can be decomposed as [13, 14]

$$L = l + z\eta, \quad (3.1)$$

where $l^2 = 0$, and η is a fixed and arbitrary null vector, $\eta^2 = 0$; z is a real number. Equation (3.1) determines z as a function of L :

$$z = \frac{L^2}{2(L\eta)}. \quad (3.2)$$

Using spinor notation, we can write l and η as $l_{\alpha\dot{\alpha}} = l_{\alpha}\tilde{l}_{\dot{\alpha}}$, $\eta_{\alpha\dot{\alpha}} = \eta_{\alpha}\tilde{\eta}_{\dot{\alpha}}$. It then follows that⁶

$$l_{\alpha} = \frac{L_{\alpha\dot{\alpha}}\tilde{\eta}^{\dot{\alpha}}}{[\tilde{l}\tilde{\eta}]}, \quad (3.3)$$

$$\tilde{l}_{\dot{\alpha}} = \frac{\eta^{\alpha}L_{\alpha\dot{\alpha}}}{\langle l\eta \rangle}. \quad (3.4)$$

We notice that (3.3) and (3.4) coincide with the CSW prescription proposed in [7] to determine the spinor variables l and \tilde{l} associated with the non-null, off-shell four-vector L defined in (3.1). The denominators on the right hand sides of (3.3) and (3.4) turn out to be irrelevant for our applications, since the expressions we will be dealing with are homogeneous in the spinor variables l_{α} ; hence we will discard them.

To proceed further, we need to re-express the usual integration measure d^4L over the loop momentum L in terms of the new variables l and z introduced previously. We found that⁷

$$\frac{d^4L}{L^2 + i\epsilon} = \frac{d\mathcal{N}(l)}{4i} \frac{dz}{z + i\epsilon}, \quad (3.5)$$

where we have introduced the Nair measure [31]

$$d\mathcal{N}(l) := \langle l dl \rangle d^2\tilde{l} - [\tilde{l} d\tilde{l}] d^2l. \quad (3.6)$$

⁶Spinor inner products are defined as $\langle \lambda \mu \rangle := \epsilon_{\alpha\beta}\lambda^{\alpha}\mu^{\beta}$, $[\tilde{\lambda} \tilde{\mu}] := \epsilon_{\dot{\alpha}\dot{\beta}}\tilde{\lambda}^{\dot{\alpha}}\tilde{\mu}^{\dot{\beta}}$.

⁷The $i\epsilon$ prescription in the left and right hand sides of (3.5) was understood in [17], and, as stressed in [13, 30], it is essential in order to correctly perform loop integrations.

Eq. (3.5) is key to the procedure. It is important to notice that the product of the measure factor with a scalar propagator $d^4L/(L^2+i\varepsilon)$ in (3.5) is independent of the reference vector η . In [31], it was noticed that the Lorentz invariant phase space measure for a massless particle can be expressed precisely in terms of the Nair measure:

$$d^4l \delta^{(+)}(l^2) = \frac{d\mathcal{N}(l)}{4i}, \quad (3.7)$$

where, as before, we write the null vector l as $l_{\alpha\dot{\alpha}} = l_\alpha \tilde{l}_{\dot{\alpha}}$, and in Minkowski space we identify $\tilde{l} = l^*$.

Next, we observe that in computing one-loop diagrams, the four-dimensional integration measure which appears is

$$d\mathcal{M} := \frac{d^4L_1}{L_1^2} \frac{d^4L_2}{L_2^2} \delta^{(4)}(L_2 - L_1 + P_L), \quad (3.8)$$

where L_1 and L_2 are loop momenta, and P_L is the external momentum flowing outside the loop⁸ so that $L_2 - L_1 + P_L = 0$. Next we express L_1 and L_2 as in (3.1),

$$L_{i;\alpha,\dot{\alpha}} = l_{i\alpha} \tilde{l}_{i\dot{\alpha}} + z_i \eta_\alpha \tilde{\eta}_{\dot{\alpha}}, \quad i = 1, 2. \quad (3.9)$$

Using (3.9), we rewrite the argument of the delta function as

$$L_2 - L_1 + P_L = l_2 - l_1 + P_{L;z}, \quad (3.10)$$

where we have defined

$$P_{L;z} := P_L - z\eta, \quad (3.11)$$

and

$$z := z_1 - z_2. \quad (3.12)$$

Notice that we use the same η for both the momenta L_1 and L_2 . Using (3.9), we can finally recast (3.8) as [17]

$$d\mathcal{M} = \frac{dz_1}{z_1} \frac{dz_2}{z_2} d\text{LIPS}(l_2, -l_1; P_{L;z}), \quad (3.13)$$

where

$$d\text{LIPS}(l_2, -l_1; P_{L;z}) := d^4l_1 \delta^{(+)}(l_1^2) d^4l_2 \delta^{(+)}(l_2^2) \delta^{(4)}(l_2 - l_1 + P_{L;z}) \quad (3.14)$$

is the two-particle Lorentz invariant phase space (LIPS) measure. The integration measure $d\mathcal{M}$ as it is expressed on the right hand side of (3.13) can now be immediately dimensionally regularised; this is accomplished by simply replacing the four-dimensional LIPS measure by its continuation to $D = 4 - 2\epsilon$ dimensions,

$$d^D\text{LIPS}(l_2, -l_1; P_{L;z}) := d^Dl_1 \delta^{(+)}(l_1^2) d^Dl_2 \delta^{(+)}(l_2^2) \delta^{(D)}(l_2 - l_1 + P_{L;z}). \quad (3.15)$$

⁸In our conventions, all external momenta are outgoing.

Eq. (3.13) was one of the key results of [17]. It gives a decomposition of the original integration measure into a D -dimensional phase space measure and a dispersive measure. According to Cutkosky's cutting rules [32], the LIPS measure computes the discontinuity of a Feynman diagram across its branch cuts. Which discontinuity is evaluated is determined by the argument of the delta function appearing in the LIPS measure; in (3.13) this is $P_{L;z}$ (defined in (3.11)). Notice that $P_{L;z}$ always contains a term proportional to the reference vector η , as prescribed by (3.11). Finally, discontinuities are integrated using the dispersive measure in (3.13), thereby reconstructing the full amplitude.

As a last remark, notice that, in contradistinction with the cut-constructibility approach of BDDK, here we sum over all the cuts – each of which is integrated with the appropriate dispersive measure.

4 MHV one-loop amplitudes in $\mathcal{N} = 1$ SYM from MHV vertices

In the last section we reviewed how MHV vertices can be sewn together into one-loop diagrams, and how a particular decomposition of the loop momentum measure leads to a representation of the amplitudes strikingly similar to traditional dispersion formulae. This method was tested successfully in [17] for the case of MHV one-loop amplitudes in $\mathcal{N} = 4$ SYM. In the following we will apply the same philosophy to amplitudes in $\mathcal{N} = 1$ SYM, in particular to the infinite sequence of MHV one-loop amplitudes, which was obtained using the cut-constructibility approach [28], and whose twistor space picture has more recently been analysed in [22].

Similarly to the $\mathcal{N} = 4$ case, the one-loop amplitude has an overall factor proportional to the MHV tree-level amplitude, but, as opposed to the $\mathcal{N} = 4$ case, the remaining one-loop factor depends non-trivially on the positions i and j of the two external negative helicity gluons. This is due to the fact that a different set of fields is allowed to propagate in the loops.

The MHV Feynman diagrams contributing to MHV one-loop amplitudes consist of two MHV vertices connected by two off-shell scalar propagators. If both negative helicity gluons are on one MHV vertex, only gluons of a particular helicity can propagate in the loop. This is independent of the number of supersymmetries. On the other hand, for diagrams with one negative helicity gluon on one MHV vertex and the other negative helicity gluon on the other MHV vertex, all components of the supersymmetric multiplet propagate in the loop. In the case of $\mathcal{N} = 4$ SYM this corresponds to helicities $h = -1, -1/2, 0, 1/2, 1$ with multiplicities 1, 4, 6, 4, 1, respectively; for the $\mathcal{N} = 1$ vector multiplet the multiplicities are 1, 1, 0, 1, 1. Hence, we can obtain the $\mathcal{N} = 1$ amplitude by simply taking the $\mathcal{N} = 4$ amplitude and subtracting three times the contribution of an

$\mathcal{N} = 1$ chiral multiplet, which has multiplicities $0, 1, 2, 1, 0$.⁹

This supersymmetric decomposition of general one-loop amplitudes is useful as it splits the calculation into pieces of increasing difficulty, and allows one to reduce a one-loop diagram with gluons circulating in the loop to a combination of an $\mathcal{N} = 4$ vector amplitude, an $\mathcal{N} = 1$ chiral amplitude and finally a non-supersymmetric amplitude with a scalar field running in the loop.

In our case, the supersymmetric decomposition takes the form

$$\mathcal{A}_n^{\mathcal{N}=1, \text{vector}} = \mathcal{A}_n^{\mathcal{N}=4} - 3 \mathcal{A}_n^{\mathcal{N}=1, \text{chiral}} , \quad (4.1)$$

where n denotes the number of external lines. Since the $\mathcal{N} = 4$ contribution is known, one needs to determine $\mathcal{A}_n^{\mathcal{N}=1, \text{chiral}}$ using MHV diagrams. To be precise, we are only addressing the computation of the planar part of the amplitudes. However this is sufficient, since at one-loop level the non-planar partial amplitudes are obtained as appropriate sums of permutations of the planar partial amplitudes [18], as discussed at the beginning of Section 3.

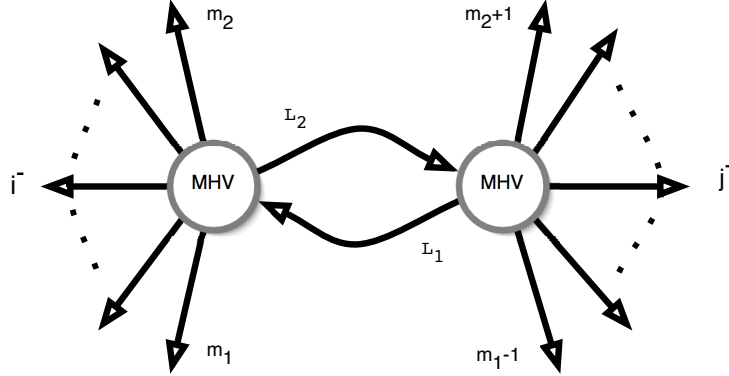


Figure 4: A one-loop MHV diagram, computed in 4.4 using MHV amplitudes as interaction vertices, with the CSW off-shell prescription. The two external gluons with negative helicity are labelled by i and j .

Therefore our task consists of

1. Evaluating the class of diagrams where we allow all the helicity states of a chiral multiplet,

$$h \in \{-1/2, 0, 0, 1/2\} , \quad (4.2)$$

to run in the loop. We depict the prototype of such diagrams in Figure 4.

⁹We can also obtain the $\mathcal{N} = 2$ amplitude in a completely similar way.

2. Summing over all diagrams such that each of the two MHV vertices always has one external gluon of negative helicity. Assigning i^- to the left and j^- to the right, the summation range of m_1 and m_2 is determined to be:

$$j + 1 \leq m_1 \leq i, \quad i \leq m_2 \leq j - 1. \quad (4.3)$$

Therefore we get

$$\begin{aligned} \mathcal{A}_n^{\mathcal{N}=1, \text{chiral}} &= \sum_{m_1, m_2, h} \int d\mathcal{M} \mathcal{A}(-l_1, m_1, \dots, i^-, \dots, m_2, l_2) \\ &\quad \cdot \mathcal{A}(-l_2, m_2 + 1, \dots, j^-, \dots, m_1 - 1, l_1), \end{aligned} \quad (4.4)$$

where the summation ranges of h , m_1 and m_2 are given in (4.2), (4.3). Notice that, in order to compute the loop amplitude (4.4), we make use of the integration measure $d\mathcal{M}$, given in (3.13), which was found in [17].

After some spinor algebra and after performing the sum over the helicities h , the integrand of (4.4) becomes

$$-i\mathcal{A}_n^{\text{tree}} \cdot \frac{\langle m_2 (m_2 + 1) \rangle \langle (m_1 - 1) m_1 \rangle \langle i l_1 \rangle \langle j l_1 \rangle \langle i l_2 \rangle \langle j l_2 \rangle}{\langle i j \rangle^2 \langle m_1 l_1 \rangle \langle (m_1 - 1) l_1 \rangle \langle m_2 l_2 \rangle \langle (m_2 + 1) l_2 \rangle}. \quad (4.5)$$

The focus of the remainder of this section will be to evaluate the integral in (4.4) explicitly. Since $-i\mathcal{A}_n^{\text{tree}}$ factors out completely, we will drop it and only reinstate it at the very end of the calculation.

The integrand (without this factor) can be rewritten in terms of dot products of momentum vectors,

$$\mathcal{I} = \frac{\mathcal{N}}{(i \cdot j)^2 (m_1 \cdot l_1) ((m_1 - 1) \cdot l_1) (m_2 \cdot l_2) ((m_2 + 1) \cdot l_2)}, \quad (4.6)$$

with

$$\mathcal{N} = \text{tr}_+ (\not{l}_1 \not{k}_{m_1-1} \not{k}_{m_1} \not{l}_1 \not{k}_j \not{k}_i) \text{tr}_+ (\not{l}_2 \not{k}_{m_2} \not{k}_{m_2+1} \not{l}_2 \not{k}_j \not{k}_i). \quad (4.7)$$

\mathcal{N} is a product of Dirac traces, where the tr_+ symbol indicates that the projector $(1 + \gamma^5)/2$ has been inserted.

Next, notice that each of these Dirac traces involving six momenta can be expressed in terms of simpler Dirac traces involving only four momenta. For the first factor of (4.7) we find

$$\text{tr}_+ (\not{l}_1 \not{k}_{m_1-1} \not{k}_{m_1} \not{l}_1 \not{k}_j \not{k}_i) = 2(m_1 \cdot l_1) \text{tr}_+ (\not{k}_i \not{k}_j \not{k}_{m_1-1} \not{l}_1) - 2((m_1 - 1) \cdot l_1) \text{tr}_+ (\not{k}_i \not{k}_j \not{k}_{m_1} \not{l}_1), \quad (4.8)$$

where

$$\text{tr}_+ (\not{k}_a \not{k}_b \not{k}_c \not{k}_d) = 2[(a \cdot b)(c \cdot d) - (a \cdot c)(b \cdot d) + (a \cdot d)(b \cdot c)] - 2i\varepsilon(a, b, c, d). \quad (4.9)$$

The second factor in (4.7) takes a similar form. Consequently, the integrand becomes a sum of four terms, one of which is

$$\frac{\text{tr}_+ (\not{k}_i \not{k}_j \not{k}_{m_1} \not{l}_1) \text{tr}_+ (\not{k}_i \not{k}_j \not{k}_{m_2} \not{l}_2)}{(i \cdot j)^2 (m_1 \cdot l_1) (m_2 \cdot l_2)}. \quad (4.10)$$

The other three terms are obtained by replacing m_1 with $m_1 - 1$ and/or m_2 with $m_2 + 1$ in (4.10) and come with alternating signs. Note that the original expression (4.5) is symmetric in i , and j , although when we make use of the decomposition (4.10) this symmetry is no longer manifest. We will symmetrize over i and j at the end of the calculation in order to make this exchange symmetry manifest in the final expression.

In the next step we have to perform the phase space integration, which is equivalent to the calculation of a unitarity cut with momentum $P_{L;z} = \sum_{l=m_1}^{m_2} k_l - z\eta$ flowing through the cut. Note that, as explained in Section 3, the momentum is shifted by a term proportional to the reference momentum η . The term $(l_1 \cdot m_1)(l_2 \cdot m_2)$ in the denominator in (4.10) corresponds to two propagators, hence the denominator by itself corresponds to a cut box diagram. However, the numerator of (4.10) depends non-trivially on the loop momentum, so that in fact (4.10) corresponds to a tensor box diagram, not simply a scalar box diagram. Using the Passarino-Veltman method [33], we can reduce the expression (4.10), integrated with the LIPS measure, to a sum of cuts of scalar box diagrams, scalar and vector triangle diagrams, and scalar bubble diagrams. This procedure is somewhat technical, and details are collected in Appendix A. Luckily, the final result takes a less intimidating form than the intermediate expressions. We will now present the result of these calculations after the LIPS integration.

We first observe that loop integrations are performed in $4 - 2\epsilon$ dimensions. It turns out that singular $1/\epsilon$ terms appearing at intermediate steps of the phase space integration cancel out completely. Notice that this does not mean that the final result will be free of infrared divergences. In fact the dispersion integral can and does give rise to $1/\epsilon$ divergent terms but there cannot be any $1/\epsilon^2$ terms, as expected for the contribution of a chiral multiplet [28]. The $1/\epsilon$ divergences in the scattering amplitude correspond to the bubble contributions in (2.2), or degenerate triangles contributions in (2.19), as explained in Section 2. In Appendix A we show that the finite terms of the phase space integral combine into the following simple expression:

$$\hat{\mathcal{C}} = \mathcal{C}(m_1 - 1, m_2) - \mathcal{C}(m_1, m_2) + \mathcal{C}(m_1, m_2 + 1) - \mathcal{C}(m_1 - 1, m_2 + 1), \quad (4.11)$$

with¹⁰

$$\begin{aligned} \mathcal{C}(m_1, m_2) &= \frac{2\pi}{1 - 2\epsilon} \frac{(P_{L;z}^2)^{-\epsilon}}{(i \cdot j)^2 (m_1 \cdot m_2)} \left[\frac{\mathcal{T}(m_1, m_2, P_{L;z})}{(m_1 \cdot P_{L;z})} + \frac{\mathcal{T}(m_2, m_1, P_{L;z})}{(m_2 \cdot P_{L;z})} \right] \\ &\quad - \frac{2\pi \mathcal{T}(m_1, m_2, m_2)}{(i \cdot j)^2 (m_1 \cdot m_2)^2} (P_{L;z}^2)^{-\epsilon} \log(1 - a_z P_{L;z}^2), \end{aligned} \quad (4.12)$$

¹⁰In (4.12) we omit an overall, finite numerical factor that depends on ϵ . This factor, which can be read off from (B.12), is irrelevant for our discussion.

where

$$\begin{aligned} \mathcal{T}(m_1, m_2, P) &:= \text{tr}_+ (k_i k_j k_{m_1} \mathcal{P}) \text{tr}_+ (k_i k_j k_{m_2} k_{m_1}) , \\ a_z &:= \frac{m_1 \cdot m_2}{N(P_{L;z})} , \end{aligned} \quad (4.13)$$

and

$$N(P) := (m_1 \cdot m_2) P^2 - 2(m_1 \cdot P)(m_2 \cdot P) . \quad (4.14)$$

A closer inspection of (4.12) reveals that the first line of that expression corresponds to two cuts of scalar triangle integrals, up to an ϵ -dependent factor and the explicit z -dependence of the two numerators. The second line is a term familiar from [17], corresponding to the $P_{L;z}^2$ -cut of the finite part B of a scalar box function, defined in (2.9) (see also (2.7)). The full result for the one-loop MHV amplitudes is obtained by summing over all possible MHV diagrams, as specified in (4.4) and (4.2), (4.3).

We begin our analysis by focusing on the box function contributions in (4.12), and notice the following important facts:

1. By taking into account the four terms in (4.11) and summing over Feynman diagrams, we see each fixed finite box function B appears in exactly four phase space integrals, one for each of its possible cuts, in complete similarity with [17]. It was shown in Section 5 of that paper that the corresponding dispersion integration over z will then yield the finite B part of the scalar box functions F . It was also noted in [17] that one can make a particular gauge choice for η such that the z -dependence in N disappears. This happens when η is chosen to be equal to one of the massless external legs of the box function. The question of gauge invariance is discussed in Appendix C.
2. The coefficient multiplying the finite box function is precisely equal to $b_{m_1, m_2}^{i, j}$ defined in (2.5).
3. Finally, the functions B generated by summing over all MHV Feynman diagrams with the range dictated by (4.3) are precisely those included in the double sum for the finite box functions in the first line of (2.2) (or (2.19)) upon identifying m_1 and m_2 with s and m . To be precise, (4.3) includes the case where the indices s and/or m (in the notation of (2.2) and (2.19)) are equal to either i or j ; but for any of these choices, it is immediate to check that the corresponding coefficient $b_{m, s}^{i, j}$ vanishes.

This settles the agreement between the result of our computation with MHV vertices and (2.19) for the part corresponding to the box functions. Next we have to collect the cuts contributing to particular triangles, and show that the z -integration reproduces the expected triangle functions from (2.19), each with the correct coefficient.

To this end, we notice that for each fixed triangle function $T(p, P, Q)$, exactly four phase space integrals appear, two for each of the two possible cuts of the function. Moreover, a gauge invariance similar to that of the box functions also exists for triangle cuts (see Appendix C), so that we can choose η in a way that the \mathcal{T} numerators in (4.12) become independent of z . A particularly convenient choice is $\eta = k_i$, since it can be kept fixed for all possible cuts. Choosing this gauge, we see that a sum, \mathbb{T} , of terms proportional to cut-triangles is generated from (4.11) (up to a common normalisation):

$$\mathbb{T} := T_A + T_B + T_C + T_D , \quad (4.15)$$

where

$$\begin{aligned} T_A &:= \left[\frac{\mathcal{S}(i, j, m_1, m_2)}{(m_1 \cdot m_2)} - \frac{\mathcal{S}(i, j, m_1 - 1, m_2)}{((m_1 - 1) \cdot m_2)} \right] \mathcal{S}(i, j, m_2, P_L) \Delta_A , \\ T_B &:= \left[\frac{\mathcal{S}(i, j, m_2, m_1)}{(m_1 \cdot m_2)} - \frac{\mathcal{S}(i, j, m_2 + 1, m_1)}{((m_2 + 1) \cdot m_1)} \right] \mathcal{S}(i, j, m_1, P_L) \Delta_B , \\ T_C &:= \left[\frac{\mathcal{S}(i, j, m_2 + 1, m_1 - 1)}{((m_2 + 1) \cdot (m_1 - 1))} - \frac{\mathcal{S}(i, j, m_2, m_1 - 1)}{(m_2 \cdot (m_1 - 1))} \right] \mathcal{S}(i, j, m_1 - 1, P_L) \Delta_C , \\ T_D &:= \left[\frac{\mathcal{S}(i, j, m_1 - 1, m_2 + 1)}{((m_1 - 1) \cdot (m_2 + 1))} - \frac{\mathcal{S}(i, j, m_1, m_2 + 1)}{(m_1 \cdot (m_2 + 1))} \right] \mathcal{S}(i, j, m_2 + 1, P_L) \Delta_D . \end{aligned} \quad (4.16)$$

Here we have defined

$$\mathcal{S}(a, b, c, d) = \text{tr}_+ (\not{k}_a \not{k}_b \not{k}_c \not{k}_d) , \quad (4.17)$$

and Δ_I , $I = A, \dots, D$, are the following cut-triangles, all in the $P_{L;z}$ -cut :

$$\begin{aligned} \Delta_A &:= \frac{1}{(m_2 \cdot P_{L;z})} = Q^2\text{-cut of } -T(m_2, P_{L;z} - m_2, -P_{L;z}) , \\ \Delta_B &:= \frac{1}{(m_1 \cdot P_{L;z})} = P^2\text{-cut of } -T(m_1, -P_{L;z}, P_{L;z} - m_1) , \\ \Delta_C &:= \frac{1}{((m_1 - 1) \cdot P_{L;z})} = Q^2\text{-cut of } T(m_1 - 1, -P_{L;z} - (m_1 - 1), P_{L;z}) , \\ \Delta_D &:= \frac{1}{((m_2 + 1) \cdot P_{L;z})} = P^2\text{-cut of } T(m_2 + 1, P_{L;z}, -P_{L;z} - (m_2 + 1)) . \end{aligned} \quad (4.18)$$

Next, we notice that the prefactors multiplying Δ_B , Δ_C become the same, up to a minus sign, upon shifting $m_1 - 1 \rightarrow m_1$ in the second prefactor; and so do the prefactors of Δ_A , Δ_D upon shifting $m_2 \rightarrow m_2 + 1$. Doing this, $-\Delta_B$ and the shifted Δ_C become the two cuts of the same triangle function $T(m_1, -P_{L;z}, P_{L;z} - m_1)$, and similarly, $-\Delta_A$ and Δ_D give the two cuts of the function $T(m_2, P_{L;z} - m_2, -P_{L;z})$. Furthermore, in Appendix C we will show that summing the two dispersion integrals of the two different cuts of a triangle indeed generates the triangle function – in fact this procedure gives a novel way

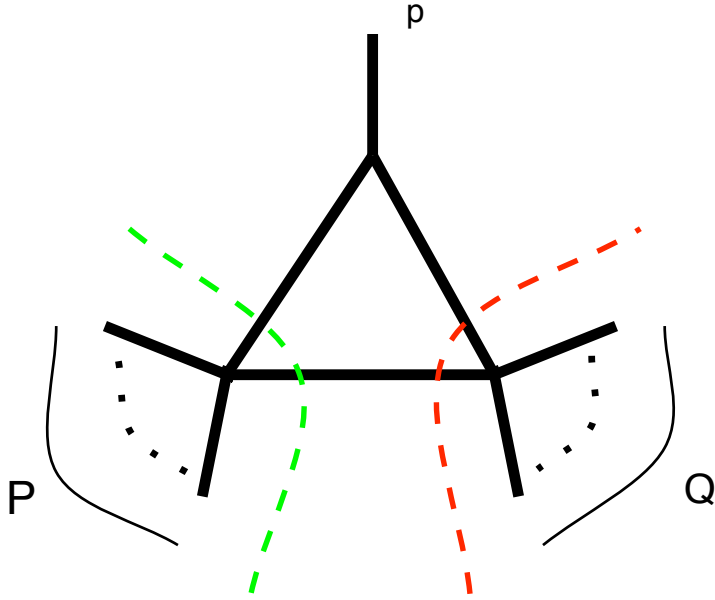


Figure 5: A triangle function with massive legs labelled by P and Q , and massless leg p . This function is reconstructed by summing two dispersion integrals, corresponding to the P_z^2 - and Q_z^2 -cut.

of obtaining the triangle functions.¹¹ Specifically, the result derived in Appendix C is

$$\int \frac{dz}{z} \left[\frac{(P_z^2)^{-\epsilon}}{(P_z p)} + \frac{(Q_z^2)^{-\epsilon}}{(Q_z p)} \right] = 2[\pi\epsilon \csc(\pi\epsilon)] T_\epsilon(p, P, Q), \quad (4.19)$$

where the ϵ -dependent triangle function $T_\epsilon(p, P, Q)$ (with $p + P + Q = 0$) was introduced in (2.14) and gives, as $\epsilon \rightarrow 0$, the triangle function (2.13) (as well as the bubbles when either P^2 or Q^2 vanish). The result (4.19) holds for a generic choice of the reference vector η , see (C.7)-(C.12). We give a pictorial representation of the non-degenerate and degenerate triangle functions in Figures 5 and 6, respectively.

At this point, it should be noticed that for a gauge choice different from $\eta = k_i$ adopted so far, the numerators \mathcal{T} in (4.12) do acquire an η -dependence. This gauge dependence should not be present in the final result for the scattering amplitude. Indeed, it is easy to check that, thanks to (C.7), the coefficient of the η -dependent terms actually vanishes.

¹¹A remark is in order here. In our procedure the momentum appearing in each of the possible cuts is always shifted by an amount proportional to $z\eta$; the triangle is then reproduced by performing the appropriate dispersion integrals. Because of the above mentioned shift, we produce a non-vanishing cut (with shifted momentum) even when the cut includes only one external (massless) leg, say \tilde{k} , as the momentum flowing in the cut is effectively $\tilde{k}_z = \tilde{k} - z\eta$, so that $\tilde{k}_z^2 \neq 0$.

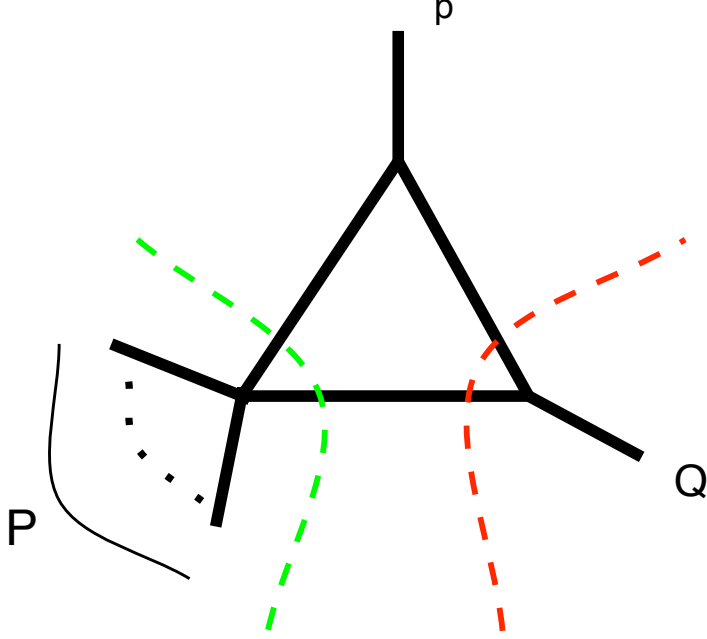


Figure 6: A degenerate triangle function. Here the leg labelled by P is still massive, but that labelled by Q becomes massless. This function is also reconstructed by summing over two dispersion integrals, corresponding to the P_z^2 - and Q_z^2 -cut.

Using now (4.15)-(4.19) and collecting terms as specified above, we see that the generic term produced by this procedure takes the form

$$\left[\frac{\mathcal{S}(i, j, a, p_m)}{(k_a \cdot p_m)} - \frac{\mathcal{S}(i, j, a + 1, p_m)}{(k_{a+1} \cdot p_m)} \right] \mathcal{S}(i, j, p_m, Q) T(p_m, P, Q) , \quad (4.20)$$

with $P = q_{a+1, m-1}$ and $Q = q_{m+1, a}$.

Finally, we implement the symmetrization of the indices i, j , as explained earlier, and convert (4.20) into

$$c_{m,a}^{i,j} T(p_m, P, Q) , \quad (4.21)$$

where the coefficient $c_{m,a}^{i,j}$ is¹²

$$c_{m,a}^{i,j} := \frac{1}{2} \left[\frac{\mathcal{S}(i, j, a + 1, p_m)}{(k_{a+1} \cdot p_m)} - \frac{\mathcal{S}(i, j, a, p_m)}{(k_a \cdot p_m)} \right] \frac{\mathcal{S}(i, j, p_m, q_{m,a}) - \mathcal{S}(i, j, q_{m,a}, p_m)}{[(k_i + k_j)^2]^2} , \quad (4.22)$$

which coincides with the definition of $c_{m,a}^{i,j}$ given in (2.6). Finally, it is easy to see that in summing over the range given by (4.3), we produce exactly all the triangle functions

¹²In writing (4.22), we make also use of the fact that $\mathcal{S}(i, j, q_{m-1, a}, p_m) = \mathcal{S}(i, j, q_{m, a}, p_m)$.

appearing in the second line of (2.19). It is also important to notice that the bubbles, which appear in the last line of (2.2), are actually obtained as particular cases of triangle functions where one of the massive legs becomes massless, as observed at the end of Section 2.

In conclusion, we have seen that all the terms in (2.19), i.e. finite box contributions and triangle contributions – which include the bubbles as special (degenerate) cases – are precisely reproduced in our diagrammatic approach.

Acknowledgements

It is a pleasure to thank Lance Dixon, Valya Khoze, David Kosower, Marco Matone and Sanjaye Ramgoolam for interesting conversations. GT acknowledges the support of PPARC.

Appendix A: Passarino-Veltman reduction

In Section 4 we saw that a typical term in the $\mathcal{N} = 1$ amplitude is the dispersion integral of the following phase space integral:

$$\mathcal{C}(m_1, m_2) := \int d\text{LIPS}(l_2, -l_1; P_{L;z}) \frac{\text{tr}_+(k_i k_j k_{m_1} \not{l}_1) \text{tr}_+(k_i k_j k_{m_2} \not{l}_2)}{(i \cdot j)^2 (m_1 \cdot l_1) (m_2 \cdot l_2)}. \quad (\text{A.1})$$

The full amplitude is then obtained by adding the dispersion integrals of three more terms similar to (A.1) but with m_1 replaced by $m_1 - 1$ and/or m_2 replaced by $m_2 + 1$. The goal of this Appendix is to perform the Passarino-Veltman reduction [33] of (A.1), which will lead us to re-express $\mathcal{C}(m_1, m_2)$ in terms of cut-boxes, cut-triangles and cut-bubbles.

The explicit forms for the Dirac traces involve Lorentz contractions over the various momenta, so in a short-hand notation we can write these as

$$T(i, j, m_1)_\mu l_1^\mu := \text{tr}_+(k_i k_j k_{m_1} \not{l}_1). \quad (\text{A.2})$$

$\mathcal{C}(m_1, m_2)$ can then be recast as

$$\mathcal{C}(m_1, m_2) = \frac{T(i, j, m_1)_\mu T(i, j, m_2)_\nu}{(i \cdot j)^2} \mathcal{I}^{\mu\nu}(m_1, m_2, P_{L;z}), \quad (\text{A.3})$$

where¹³

$$\mathcal{I}^{\mu\nu}(m_1, m_2, P_L) = \int d\text{LIPS}(l_2, -l_1; P_L) \frac{l_1^\mu l_2^\nu}{(m_1 \cdot l_1)(m_2 \cdot l_2)}. \quad (\text{A.4})$$

$\mathcal{I}^{\mu\nu}(m_1, m_2, P_L)$ contains three independent momenta m_1 , m_2 and P_L . On general grounds, we can therefore decompose it as

$$\begin{aligned} \mathcal{I}^{\mu\nu} &= \eta^{\mu\nu} \mathcal{I}_0 + m_1^\mu m_1^\nu \mathcal{I}_1 + m_2^\mu m_2^\nu \mathcal{I}_2 + P_L^\mu P_L^\nu \mathcal{I}_3 + m_1^\mu m_2^\nu \mathcal{I}_4 \\ &+ m_2^\mu m_1^\nu \mathcal{I}_5 + m_1^\mu P_L^\nu \mathcal{I}_6 + P_L^\mu m_1^\nu \mathcal{I}_7 + m_2^\mu P_L^\nu \mathcal{I}_8 + P_L^\mu m_2^\nu \mathcal{I}_9, \end{aligned} \quad (\text{A.5})$$

for some coefficients $\mathcal{I}_i, i = 0, \dots, 9$. One can then contract with different combinations of the independent momenta in order to solve for the \mathcal{I}_i . For instance, two of the integrals that we will end up having to do are $\eta^{\mu\nu} \mathcal{I}_{\mu\nu}$ and $m_1^\mu m_1^\nu \mathcal{I}_{\mu\nu}$. Using momentum conservation $l_2 - l_1 + P_L = 0$ and the identity $a \cdot b = (a + b)^2/2 = -(a - b)^2/2$ for a, b massless momenta, we can convert these integrals into ones which have the general form

$$\tilde{\mathcal{I}}^{(a,b)} = \int \frac{d\text{LIPS}(l_2, -l_1; P_L)}{(l_1 \cdot m_1)^a (l_2 \cdot m_2)^b}, \quad (\text{A.6})$$

possibly with a kinematical-invariant coefficient, and with a and b ranging over the values $1, 0, -1$. The results of these integrals are collected in Appendix B. As an example, we find that

$$m_1^\mu m_1^\nu \mathcal{I}_{\mu\nu} = \int d\text{LIPS}(l_2, -l_1; P_L) \frac{(l_1 \cdot m_1)}{(l_2 \cdot m_2)} - (m_1 \cdot P_L) \int \frac{d\text{LIPS}(l_2, -l_1; P_L)}{(l_2 \cdot P_L)}. \quad (\text{A.7})$$

¹³For the rest of this Appendix we drop the subscript z in $P_{L;z}$ for the sake of brevity.

Considering the values (a, b) , the case $(1, 1)$ is a cut scalar box, $(1, 0)$ and $(0, 1)$ are cut scalar triangles, $(1, -1)$ and $(-1, 1)$ are cut vector triangles, whilst $(0, 0)$ is a cut scalar bubble.

Because of the structure of $T(i, j, m_1)_\mu$ and $T(i, j, m_2)_\nu$, terms with coefficients such as $T(i, j, m_1)_\mu T(i, j, m_2)_\nu m_1^\mu m_2^\nu$ are zero, and thus some of the \mathcal{I}_i do not contribute to the final answer. The only contributing terms are found to be \mathcal{I}_3 , \mathcal{I}_5 , \mathcal{I}_7 and \mathcal{I}_8 , and we find that

$$\begin{aligned}
\mathcal{C}(m_1, m_2) &= \frac{\text{tr}_+(k_i k_j k_{m_1} \not{P}_L) \text{tr}_+(k_i k_j k_{m_2} \not{P}_L)}{(i \cdot j)^2} \mathcal{I}_3 \\
&+ \frac{\text{tr}_+(k_i k_j k_{m_1} k_{m_2}) \text{tr}_+(k_i k_j k_{m_2} k_{m_1})}{(i \cdot j)^2} \mathcal{I}_5 \\
&+ \frac{\text{tr}_+(k_i k_j k_{m_1} \not{P}_L) \text{tr}_+(k_i k_j k_{m_2} k_{m_1})}{(i \cdot j)^2} \mathcal{I}_7 \\
&+ \frac{\text{tr}_+(k_i k_j k_{m_1} k_{m_2}) \text{tr}_+(k_i k_j k_{m_2} \not{P}_L)}{(i \cdot j)^2} \mathcal{I}_8 .
\end{aligned} \tag{A.8}$$

The inversion of (A.5) in order to find the coefficients is tedious and somewhat lengthy, so we just present the results for the relevant \mathcal{I}_i in (A.8) above:

$$\begin{aligned}
\mathcal{I}_3 &= \frac{1}{N^2} \left\{ 2(m_1 \cdot m_2) P_L^2 \tilde{\mathcal{I}}^{(0,0)} - N(m_1 \cdot P_L) \tilde{\mathcal{I}}^{(1,0)} + N(m_2 \cdot P_L) \tilde{\mathcal{I}}^{(0,1)} \right. \\
&\left. + 2(m_2 \cdot P_L)^2 \tilde{\mathcal{I}}^{(-1,1)} + 2(m_1 \cdot P_L)^2 \tilde{\mathcal{I}}^{(1,-1)} \right\} ,
\end{aligned} \tag{A.9}$$

$$\begin{aligned}
\mathcal{I}_5 &= \frac{1}{(m_1 \cdot m_2)^2 N^2} \left\{ \left[4(m_1 \cdot P_L)^2 (m_2 \cdot P_L)^2 - 6(m_1 \cdot P_L)(m_2 \cdot P_L)(m_1 \cdot m_2) P_L^2 \right. \right. \\
&+ \left. \left. 3(m_1 \cdot m_2)^2 (P_L^2)^2 \right] \tilde{\mathcal{I}}^{(0,0)} + \left[2(m_1 \cdot P_L)^2 (m_2 \cdot P_L) - \frac{3}{2}(m_1 \cdot m_2) P_L^2 \right] N(m_1 \cdot P_L) \tilde{\mathcal{I}}^{(1,0)} \right. \\
&- \left[2(m_1 \cdot P_L)^2 (m_2 \cdot P_L) - \frac{3}{2}(m_1 \cdot m_2) P_L^2 \right] N(m_2 \cdot P_L) \tilde{\mathcal{I}}^{(0,1)} + \frac{N^3}{4} \tilde{\mathcal{I}}^{(1,1)} \\
&+ 2 \left[(m_1 \cdot m_2) P_L^2 - (m_1 \cdot P_L)(m_2 \cdot P_L) \right] (m_2 \cdot P_L)^2 \tilde{\mathcal{I}}^{(-1,1)} \\
&\left. + 2 \left[(m_1 \cdot m_2) P_L^2 - (m_1 \cdot P_L)(m_2 \cdot P_L) \right] (m_1 \cdot P_L)^2 \tilde{\mathcal{I}}^{(1,-1)} \right\} ,
\end{aligned} \tag{A.10}$$

$$\begin{aligned}
\mathcal{I}_7 &= \frac{1}{(m_1 \cdot P_L)(m_1 \cdot m_2) N^2} \left\{ \left[2(m_1 \cdot P_L)^2 (m_2 \cdot P_L)^2 - 3(m_1 \cdot P_L)(m_2 \cdot P_L)(m_1 \cdot m_2) P_L^2 \right] \right. \\
&\cdot \tilde{\mathcal{I}}^{(0,0)} + \frac{1}{2}(m_1 \cdot m_2) P_L^2 N(m_1 \cdot P_L) \tilde{\mathcal{I}}^{(1,0)} - (m_1 \cdot P_L) N(m_2 \cdot P_L)^2 \tilde{\mathcal{I}}^{(0,1)} \\
&\left. - 2(m_1 \cdot P_L)(m_2 \cdot P_L)^3 \tilde{\mathcal{I}}^{(-1,1)} - (m_1 \cdot m_2) P_L^2 (m_1 \cdot P_L)^2 \tilde{\mathcal{I}}^{(1,-1)} \right\} ,
\end{aligned} \tag{A.11}$$

$$\begin{aligned}
\mathcal{I}_8 = & \frac{1}{(m_2 \cdot P_L)(m_1 \cdot m_2)N^2} \left\{ \left[2(m_1 \cdot P_L)^2(m_2 \cdot P_L)^2 - 3(m_1 \cdot P_L)(m_2 \cdot P_L)(m_1 \cdot m_2)P_L^2 \right] \right. \\
& \cdot \tilde{\mathcal{I}}^{(0,0)} + (m_2 \cdot P_L)N(m_1 \cdot P_L)^2 \tilde{\mathcal{I}}^{(1,0)} - \frac{1}{2}(m_1 \cdot m_2)P_L^2 N(m_2 \cdot P_L) \tilde{\mathcal{I}}^{(0,1)} \\
& \left. - (m_1 \cdot m_2)P_L^2(m_2 \cdot P_L)^2 \tilde{\mathcal{I}}^{(-1,1)} - 2(m_1 \cdot P_L)^3(m_2 \cdot P_L) \tilde{\mathcal{I}}^{(1,-1)} \right\}, \tag{A.12}
\end{aligned}$$

where $N = (m_1 \cdot m_2)P_L^2 - 2(m_1 \cdot P_L)(m_2 \cdot P_L)$. The explicit expressions for the relevant $\tilde{\mathcal{I}}^{(a,b)}$ are summarised in Appendix B.

Combining (A.8) and (A.9)-(A.12) with the identity (D.7) and the explicit expressions for the integrals $\tilde{\mathcal{I}}^{(a,b)}$ in Appendix B, we arrive at the final result (4.12).

Appendix B: Box and triangle discontinuities from phase-space integrals

The integrals that arise in the Passarino-Veltman reduction in Appendix A have the general form:

$$\tilde{\mathcal{I}}^{(a,b)} = \int \frac{d^{4-2\epsilon} \text{LIPS}(l_2, -l_1; P_{L;z})}{(l_1 \cdot m_1)^a (l_2 \cdot m_2)^b}, \tag{B.1}$$

where we have introduced dimensional regularisation in dimension $D = 4 - 2\epsilon$ [34] in order to deal with infrared divergences.

There are six cases to deal with: $\tilde{\mathcal{I}}^{(0,0)}$, $\tilde{\mathcal{I}}^{(1,0)}$, $\tilde{\mathcal{I}}^{(0,1)}$, $\tilde{\mathcal{I}}^{(1,1)}$, $\tilde{\mathcal{I}}^{(-1,1)}$, $\tilde{\mathcal{I}}^{(1,-1)}$, though due to symmetry we can transform $\tilde{\mathcal{I}}^{(1,0)}$ into $\tilde{\mathcal{I}}^{(0,1)}$, and $\tilde{\mathcal{I}}^{(-1,1)}$ into $\tilde{\mathcal{I}}^{(1,-1)}$, so we only need consider four cases overall.

Generically we will evaluate these integrals in convenient special frames following Appendix B of [17], with a convenient choice for m_1 and m_2 . For instance, in the case of $\tilde{\mathcal{I}}^{(1,1)}$ it is convenient to transform to the centre of mass frame of the vector $l_1 - l_2$, so that

$$l_1 = \frac{1}{2}P_{L;z}(1, \mathbf{v}), \quad l_2 = \frac{1}{2}P_{L;z}(-1, \mathbf{v}), \tag{B.2}$$

and write

$$\mathbf{v} = (\sin \theta_1 \cos \theta_2, \dots, \cos \theta_1). \tag{B.3}$$

Using a further spatial rotation we write

$$m_1 = (m_1, 0, 0, m_1), \quad m_2 = (A, B, 0, C), \tag{B.4}$$

with the mass-shell condition $A^2 = B^2 + C^2$.

After integrating over all angular coordinates except θ_1 and θ_2 , the two-body phase space measure in $4 - 2\epsilon$ dimensions becomes [17]

$$d^{4-2\epsilon}\text{LIPS}(l_2, -l_1; P_{L;z}) = \frac{\pi^{\frac{1}{2}-\epsilon}}{4\Gamma(\frac{1}{2}-\epsilon)} \left| \frac{P_{L;z}}{2} \right|^{-2\epsilon} d\theta_1 d\theta_2 (\sin\theta_1)^{1-2\epsilon} (\sin\theta_2)^{-2\epsilon}. \quad (\text{B.5})$$

As a result of this and of our parametrizations of l_1, l_2, m_1 and m_2 , the integrals take the form

$$\tilde{\mathcal{I}}^{(a,b)} = \Lambda^{(a,b)} \frac{\pi^{\frac{1}{2}-\epsilon}}{4\Gamma(\frac{1}{2}-\epsilon)} \left| \frac{P_{L;z}}{2} \right|^{-2\epsilon} \mathcal{J}^{(a,b)}, \quad (\text{B.6})$$

where

$$\begin{aligned} \Lambda^{(0,0)} &= 1, \\ \Lambda^{(1,0)} &= \frac{2}{P_{L;z}m_1}, \\ \Lambda^{(0,1)} &= -\frac{2}{P_{L;z}m_2}, \\ \Lambda^{(1,1)} &= -\frac{4}{P_{L;z}^2m_1}, \\ \Lambda^{(-1,1)} &= -m_1, \\ \Lambda^{(1,-1)} &= -m_2, \end{aligned} \quad (\text{B.7})$$

and $\mathcal{J}^{(a,b)}$ is the angular integral

$$\mathcal{J}^{(a,b)} := \int_0^\pi d\theta_1 \int_0^{2\pi} d\theta_2 \frac{(\sin\theta_1)^{1-2\epsilon} (\sin\theta_2)^{-2\epsilon}}{(1 - \cos\theta_1)^a (A + C \cos\theta_1 + B \sin\theta_1 \cos\theta_2)^b}. \quad (\text{B.8})$$

The integrals (B.8) have been evaluated in [35] for the values of a and b specified above, and we borrow the results in a form from [36]:

$$\begin{aligned} \mathcal{J}^{(0,0)} &= \frac{2\pi}{1-2\epsilon}, \\ \mathcal{J}^{(1,0)} &= -\frac{\pi}{\epsilon}, \\ \mathcal{J}^{(1,1)} &= -\frac{\pi}{\epsilon} \frac{1}{A} {}_2F_1\left(1, 1, 1-\epsilon, \frac{A-C}{2A}\right), \\ \mathcal{J}^{(-1,1)} &= -\frac{2\pi(1-\epsilon)}{\epsilon(1-2\epsilon)} {}_2F_1\left(-1, 1, 1-\epsilon, \frac{A-C}{2A}\right). \end{aligned} \quad (\text{B.9})$$

Here, A and B will differ depending on which case we are considering and our particular parametrization for it, but in all cases the combinations that arise can be re-expressed in terms of Lorentz-invariant quantities using suitable identities. In the case of $\mathcal{J}^{(1,1)}$ for example, one uses the easily verified identities

$$N(P_{L;z}) = -P_{L;z}^2(A+C)m_1, \quad m_1 \cdot m_2 = m_1(A-C), \quad (\text{B.10})$$

where $N(P_{L;z})$ was defined in (4.14).

Eventually, after re-expressing A and B in this way, and upon application of some standard hypergeometric identities we find the following:

$$\begin{aligned}
\lambda^{-1} \tilde{\mathcal{I}}^{(0,0)} &= \frac{2\pi}{1-2\epsilon}, \\
\lambda^{-1} \tilde{\mathcal{I}}^{(1,0)} &= -\frac{1}{\epsilon} \frac{2\pi}{m_1 \cdot P_{L;z}}, \\
\lambda^{-1} \tilde{\mathcal{I}}^{(0,1)} &= \frac{1}{\epsilon} \frac{2\pi}{m_2 \cdot P_{L;z}}, \\
\lambda^{-1} \tilde{\mathcal{I}}^{(1,1)} &= -\frac{8\pi}{N(P_{L;z})} \left\{ \frac{1}{\epsilon} + \log \left(1 - \frac{(m_1 \cdot m_2) P_{L;z}^2}{N(P_{L;z})} \right) + \mathcal{O}(\epsilon) \right\}, \\
\lambda^{-1} \tilde{\mathcal{I}}^{(-1,1)} &= \frac{\pi}{(m_1 \cdot P_{L;z})^2} \left\{ -\frac{N(P_{L;z})}{\epsilon} \right. \\
&\quad \left. + \frac{2}{1-2\epsilon} [(m_1 \cdot P_{L;z})(m_2 \cdot P_{L;z}) - (m_1 \cdot m_2) P_{L;z}^2] \right\}, \\
\lambda^{-1} \tilde{\mathcal{I}}^{(1,-1)} &= \frac{\pi}{(m_2 \cdot P_{L;z})^2} \left\{ -\frac{N(P_{L;z})}{\epsilon} \right. \\
&\quad \left. + \frac{2}{1-2\epsilon} [(m_1 \cdot P_{L;z})(m_2 \cdot P_{L;z}) - (m_1 \cdot m_2) P_{L;z}^2] \right\},
\end{aligned} \tag{B.11}$$

where λ is the ubiquitous factor

$$\lambda := \frac{\pi^{\frac{1}{2}-\epsilon}}{4\Gamma(\frac{1}{2}-\epsilon)} \left| \frac{P_{L;z}}{2} \right|^{-2\epsilon}. \tag{B.12}$$

Appendix C: Reconstructing triangles from dispersion integrals in a gauge-invariant way

In this Appendix we find a new representation of the triangle function

$$T(p, P, Q) = \frac{\log(Q^2/P^2)}{Q^2 - P^2}, \tag{C.1}$$

as the dispersion integral of a sum of two cut-triangles.¹⁴ A comment on gauge-(in)dependence is in order here. Recall from Section 2, Eq. (3.1), that in the approach of [17] to loop diagrams one introduces an arbitrary null vector η in order to perform loop integrations. The corresponding gauge dependence should disappear in the expression for scattering amplitudes. In what follows we will work in an arbitrary gauge, and show analytically

¹⁴For a review of dispersion relations, see [37].

that gauge-dependent terms disappear in the final result for the triangle function. Perhaps unsurprisingly, this gauge invariance will also hold for the finite- ϵ version of $T(p, P, Q)$, which we define in (2.14).

To begin with, recall from (4.18) that the basic quantity we have to compute reads

$$\mathcal{R} := \int \frac{dz}{z} \left[\frac{(P_z^2)^{-\epsilon}}{(P_z p)} + \frac{(Q_z^2)^{-\epsilon}}{(Q_z p)} \right], \quad (\text{C.2})$$

where $P + Q + p = 0$. We will work in an arbitrary gauge, where

$$P_z := P - z\eta, \quad Q_z := Q + z\eta. \quad (\text{C.3})$$

A short calculation shows that

$$P_z p = Pp \left[1 - b_P(P^2 - P_z^2) \right], \quad (\text{C.4})$$

$$Q_z p = Qp \left[1 - b_Q(Q^2 - Q_z^2) \right], \quad (\text{C.5})$$

where

$$b_P := \frac{\eta p}{2(\eta P)(pP)}, \quad b_Q := \frac{\eta p}{2(\eta Q)(pQ)}. \quad (\text{C.6})$$

It is also useful to notice the relation

$$\frac{1}{b_Q} = \frac{1}{b_P} + Q^2 - P^2, \quad (\text{C.7})$$

as well as $(Pp) = -(Qp) = (1/2)(Q^2 - P^2)$, which trivially follows from momentum conservation. We can then rewrite (C.2) as

$$\mathcal{R} = \mathcal{I}_1 - \mathcal{I}_2, \quad (\text{C.8})$$

where

$$\begin{aligned} \mathcal{I}_1 &:= \frac{1}{(Pp)} \int ds' (s')^{-\epsilon} \frac{1}{(s' - P^2)[1 - b_P(P^2 - s')]} \\ &= \frac{\pi \csc(\pi\epsilon)}{(Pp)} \left[(-P^2)^{-\epsilon} - \left(\frac{-b_P}{b_P P^2 - 1} \right)^\epsilon \right], \end{aligned} \quad (\text{C.9})$$

$$\begin{aligned} \mathcal{I}_2 &:= \frac{1}{(Pp)} \int ds' (s')^{-\epsilon} \frac{1}{(s' - Q^2)[1 - b_Q(Q^2 - s')]} \\ &= \frac{\pi \csc(\pi\epsilon)}{(Pp)} \left[(-Q^2)^{-\epsilon} - \left(\frac{-b_Q}{b_Q Q^2 - 1} \right)^\epsilon \right]. \end{aligned} \quad (\text{C.10})$$

But (C.7) implies

$$\frac{-b_P}{b_P P^2 - 1} = \frac{-b_Q}{b_Q Q^2 - 1}, \quad (\text{C.11})$$

so that we can finally recast (C.2) as:

$$\mathcal{R} = 2[\pi\epsilon \csc(\pi\epsilon)] \frac{1}{\epsilon} \frac{(-P^2)^{-\epsilon} - (-Q^2)^{-\epsilon}}{Q^2 - P^2} = 2[\pi\epsilon \csc(\pi\epsilon)] T_\epsilon(p, P, Q), \quad (\text{C.12})$$

where the ϵ -dependent triangle function is¹⁵

$$T_\epsilon(p, P, Q) := \frac{1}{\epsilon} \frac{(-P^2)^{-\epsilon} - (-Q^2)^{-\epsilon}}{Q^2 - P^2}. \quad (\text{C.13})$$

This is the result we were after. Notice that all the gauge dependence, i.e. any dependence on the arbitrary null vector η , has completely cancelled out in (C.12).

We now discuss the $\epsilon \rightarrow 0$ limit of the final expression (C.12). As already discussed in Section 2 (see (2.15) and (2.16)), in studying the $\epsilon \rightarrow 0$ limit of \mathcal{R} (and hence of $T_\epsilon(p, P, Q)$) we need to distinguish the case where P^2 and Q^2 are both nonvanishing from the case where one of the two, say Q^2 , vanishes. In the former case, we get precisely the triangle function $T(p, P, Q)$ defined in (C.1):

$$\lim_{\epsilon \rightarrow 0} \mathcal{R} = 2T(p, P, Q), \quad P^2 \neq 0, Q^2 \neq 0. \quad (\text{C.14})$$

In the latter case, where $Q^2 = 0$, we have instead

$$\lim_{\epsilon \rightarrow 0} \mathcal{R} = -\frac{2}{\epsilon} \frac{(-P^2)^{-\epsilon}}{P^2}, \quad P^2 \neq 0, Q^2 = 0, \quad (\text{C.15})$$

which corresponds to a degenerate triangle.

The final issue is that of the gauge invariance of the contributions to the amplitude from the box functions B (this is also relevant to the issue of gauge invariance in the $\mathcal{N} = 4$ calculation of [17], and in that paper we also gave a general argument for gauge invariance). We expect that an explicit analytic proof of the gauge invariance of the box function contribution to the amplitude could be constructed using identities such as those in Appendix B of [17]. In the meantime, numerical tests have shown that gauge invariance is present [30]. Indeed, it would be surprising if this were not the case, given that the correct, gauge invariant, amplitudes are derived with the choices of gauge we have made here and in [17]. We have also carried out the MHV diagram analysis of this paper using the alternative gauge choice $\eta = k_{m_2}$; one obtains (2.19).

Appendix D: Spinor and Dirac-trace identities

In this appendix we present some identities that are needed for many of the manipulations required to massage the $\mathcal{N} = 1$ amplitude into the form given by BDDK (2.2).

¹⁵The ϵ -dependent triangle function already appeared in (2.14).

For spinor manipulations, the Schouten identity is very useful:

$$\langle i j \rangle \langle k l \rangle = \langle i k \rangle \langle j l \rangle + \langle i l \rangle \langle k j \rangle . \quad (\text{D.1})$$

Furthermore we have:

$$\langle i j \rangle [j i] = \text{tr}_+(k_i k_j) = 2(k_i \cdot k_j) , \quad (\text{D.2})$$

$$\langle i j \rangle [j l] \langle l m \rangle [m i] = \text{tr}_+(k_i k_j k_l k_m) , \quad (\text{D.3})$$

$$\langle i j \rangle [j l] \langle l m \rangle [m n] \langle n p \rangle [p i] = \text{tr}_+(k_i k_j k_l k_m k_n k_p) , \quad (\text{D.4})$$

for momenta $k_i, k_j, k_l, k_m, k_n, k_p$. For a nice introduction to the spinor helicity formalism, see [38].

For dealing with Dirac traces, the following identities are useful:

$$\text{tr}_+(k_i k_j k_l k_m) = \text{tr}_+(k_m k_l k_j k_i) , \quad (\text{D.5})$$

$$\text{tr}_+(k_i k_j k_l k_m) = 4(k_i \cdot k_j)(k_l \cdot k_m) - \text{tr}_+(k_j k_i k_l k_m) , \quad (\text{D.6})$$

for similarly generic momenta. If k_i, k_j, k_{m_1} and k_{m_2} are massless, while P_L is not necessarily so, then we have the remarkable identity:

$$\begin{aligned} & 2(k_{m_1} \cdot k_{m_2}) \text{tr}_+(k_i k_j k_{m_1} \not{P}_L) \text{tr}_+(k_i k_j k_{m_2} \not{P}_L) \\ & + P_L^2 \text{tr}_+(k_i k_j k_{m_1} k_{m_2}) \text{tr}_+(k_i k_j k_{m_2} k_{m_1}) \\ & - 2(k_{m_1} \cdot P_L) \text{tr}_+(k_i k_j k_{m_1} k_{m_2}) \text{tr}_+(k_i k_j k_{m_2} \not{P}_L) \\ & - 2(k_{m_2} \cdot P_L) \text{tr}_+(k_i k_j k_{m_1} \not{P}_L) \text{tr}_+(k_i k_j k_{m_2} k_{m_1}) = 0 . \end{aligned} \quad (\text{D.7})$$

References

- [1] E. Witten, *Perturbative gauge theory as a string theory in twistor space*, hep-th/0312171.
- [2] S. J. Parke and T. R. Taylor, *An Amplitude For N Gluon Scattering*, Phys. Rev. Lett. **56** (1986) 2459.
- [3] F. A. Berends and W. T. Giele, *Recursive Calculations For Processes With N Gluons*, Nucl. Phys. B **306** (1988) 759.
- [4] R. Roiban, M. Spradlin and A. Volovich, *A googly amplitude from the B-model in twistor space*, JHEP **0404** (2004) 012, hep-th/0402016.
- [5] R. Roiban and A. Volovich, *All googly amplitudes from the B-model in twistor space*, hep-th/0402121.
- [6] R. Roiban, M. Spradlin and A. Volovich, *On the tree-level S-matrix of Yang-Mills theory*, Phys. Rev. D **70** (2004) 026009, hep-th/0403190.
- [7] F. Cachazo, P. Svrcek and E. Witten, *MHV vertices and tree amplitudes in gauge theory*, JHEP **0409** (2004) 006, hep-th/0403047.
- [8] S. Gukov, L. Motl and A. Neitzke, *Equivalence of twistor prescriptions for super Yang-Mills*, hep-th/0404085.
- [9] C. J. Zhu, *The googly amplitudes in gauge theory*, JHEP **0404** (2004) 032, hep-th/0403115.
- [10] G. Georgiou and V. V. Khoze, *Tree amplitudes in gauge theory as scalar MHV diagrams*, JHEP **0405** (2004) 070, hep-th/0404072.
- [11] J-B. Wu and C-J Zhu, *MHV Vertices and Scattering Amplitudes in Gauge Theory*, hep-th/0406085.
- [12] J-B. Wu and C-J Zhu, *MHV Vertices and Fermionic Scattering Amplitudes in Gauge Theory with Quarks and Gluinos*, hep-th/0406146.
- [13] I. Bena, Z. Bern and D. A. Kosower, *Twistor-space recursive formulation of gauge theory amplitudes*, hep-th/0406133.
- [14] D. Kosower, *Next-to-Maximal Helicity Violating Amplitudes in Gauge Theory*, hep-th/0406175.
- [15] G. Georgiou, E. W. N. Glover and V. V. Khoze, *Non-MHV Tree Amplitudes in Gauge Theory*, JHEP **0407**, 048 (2004), hep-th/0407027.

- [16] V.V. Khoze, *Gauge Theory Amplitudes, Scalar Graphs and Twistor Space*, To appear in *From Fields to Strings: Circumnavigating Theoretical Physics*, in memory of Ian Kogan, [hep-th/0408233](#).
- [17] A. Brandhuber, B. Spence and G. Travaglini, *One-Loop Gauge Theory Amplitudes in $N=4$ super Yang-Mills from MHV Vertices*, to appear in Nucl. Phys. B, [hep-th/0407214](#)
- [18] Z. Bern, L. J. Dixon, D. C. Dunbar and D. A. Kosower, *One Loop N Point Gauge Theory Amplitudes, Unitarity And Collinear Limits*, Nucl. Phys. B **425** (1994) 217, [hep-ph/9403226](#).
- [19] N. Berkovits, *An Alternative String Theory in Twistor Space for $N = 4$ Super-Yang-Mills*, [hep-th/0402045](#).
- [20] N. Berkovits and L. Motl, *Cubic Twistorial String Field Theory*, J. High Energy Phys. **0404** (2004) 056, [hep-th/0403187](#).
- [21] N. Berkovits and E. Witten, *Conformal Supergravity in Twistor-String Theory*, [hep-th/0406051](#).
- [22] F. Cachazo, P. Svrcek and E. Witten, *Twistor space structure of one loop amplitudes in gauge theory*, [hep-th/0406177](#).
- [23] F. Cachazo, P. Svrcek and E. Witten, *Gauge Theory Amplitudes In Twistor Space And Holomorphic Anomaly*, [hep-th/0409245](#).
- [24] I. Bena, Z. Bern, D. A. Kosower and R. Roiban, *Loops in Twistor Space*, [hep-th/0410054](#).
- [25] F. Cachazo, *Holomorphic Anomaly Of Unitarity Cuts And One-Loop Gauge Theory Amplitudes*, [hep-th/0410077](#).
- [26] R. Britto, F. Cachazo, B. Feng, *Computing One-Loop Amplitudes from the Holomorphic Anomaly of Unitary Cuts*, [hep-th/0410179](#).
- [27] Z. Bern, V. Del Duca, L. J. Dixon, and D. A. Kosower, *All Non-Maximally-Helicity-Violating One-Loop Seven-Gluon Amplitudes in $N=4$ Super Yang-Mills Theory*, [hep-th/0410224](#).
- [28] Z. Bern, L. J. Dixon, D. C. Dunbar and D. A. Kosower, *Fusing gauge theory tree amplitudes into loop amplitudes*, Nucl. Phys. B **435** (1995) 59, [hep-ph/9409265](#).
- [29] T. Binoth, J. P. Guillet and G. Heinrich, *Reduction formalism for dimensionally regulated one-loop N -point*, Nucl. Phys. B **572** (2000) 361, [hep-ph/9911342](#).
- [30] L. J. Dixon, *private communication*.

- [31] V. P. Nair, *A Current Algebra For Some Gauge Theory Amplitudes*, Phys. Lett. B **214** (1988) 215.
- [32] R. E. Cutkosky, *Singularities And Discontinuities Of Feynman Amplitudes*, J. Math. Phys. **1** (1960) 429.
- [33] G. Passarino and M. J. G. Veltman, *One Loop Corrections For $E^+ E^-$ Annihilation Into $Mu^+ Mu^-$ In The Weinberg Model*, Nucl. Phys. B **160**, 151 (1979).
- [34] G. 't Hooft and M. J. G. Veltman, *Regularization And Renormalization Of Gauge Fields*, Nucl. Phys. B **44** (1972) 189.
- [35] W. L. van Neerven, *Dimensional Regularization Of Mass And Infrared Singularities In Two Loop On-Shell Vertex Functions*, Nucl. Phys. B **268** (1986) 453.
- [36] W. Beenakker, H. Kuijf, W. L. van Neerven and J. Smith, *QCD Corrections To Heavy Quark Production In P Anti- P Collisions*, Phys. Rev. D **40** (1989) 54.
- [37] R. J. Eden, P. V. Landshoff, D. I. Olive and J. C. Polkinghorne, *The Analytic S-Matrix*, Cambridge University Press, 1966.
- [38] L. J. Dixon, *Calculating scattering amplitudes efficiently*, TASI Lectures 1995, hep-ph/9601359.